Lattice QCD at finite temperature

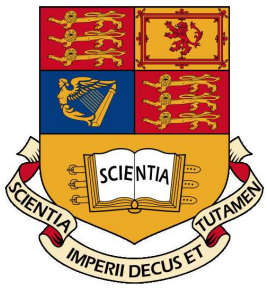

Kees Jan de Vries

Department of Theoretical Physics

Imperial College London

Submitted in partial fulfilment of the requirements for the degree of Master of Science of Imperial College London

23th of September 2011

Abstract

QCD is generally accepted to be the theory describing strong interactions. It has had tremendous successes in predicting cross sections in particle collider experiments, where the coupling constant is small. However, other phenomena at lower energies and finite temperature, such as the confinement and mass spectra of hadrons, need a non perturbative approach. QCD on the lattice is very successful an has become a standard tool in elementary particle physics. In this work I investigate a phase transition in the confinement of heavy quarks at finite temperature. I find signs of coexisting phases near the phase transition, which is compatible with the claim that the phase transition is first order.

Acknowledgements

First and above all I would like to thank my parents. They have made it possible to have this fantastic year at Imperial College London. Without their unconditional support this year would have been at least much more difficult if at all possible.

In the perspective of this dissertation, I would like to thank my supervisor Arttu Rajantie. He has given important suggestions of how to proceed in many stages of my work. I would also like to thank David Weir, who was always there for emerging questions. Thanks as well to my course mates, and in particular Benjamin, for our fruitful discussions and for proofreading this work.

Finally I would like to express my gratitude that I could use the script by Michael Creutz, which provided me with a head start for the programming part.

Contents

Chapter 1

Introduction

QCD is generally accepted to be the theory describing strong interactions. The dynamics in the vacuum and high energies is tremendously well described by means of perturbative calculations. Another exciting field of research is QCD at high energies and density. Physically we expect these conditions in heavy ion collisions, e.g. and the LHC, and in neutron stars. This study requires a non perturbative approach, for example lattice QCD. It turns out that at high enough temperature, a phase transition occurs and quarks get deconfined[1].

In this work I study this phase transition in the confinement of heavy quarks at finite temperature, much like the way it was done for the $SU(2)$ case [2]. In order to investigate the phase transition in the confinement I will define and calculate an order parameter which measures confinement. It will turn out that the order parameter is given by a thermal expectation value of a quantity P which is completely expressed in terms of gauge fields. We will see that this allows for calculating it numerically on the lattice.

In chapter 2 I give the path integral expression for the thermal expectation value. Crucially it is formulated in terms of a discretised Euclidean action.

Chapter 3 is dedicated to representing the gauge field on the lattice. An expression is derived for the discretised Euclidean action.

Once this is understood, I derive in chapter 4 that P (the Polyakov loop) measures the confinement of a single heavy quark. I explain how confinement can be understood in terms of centre symmetry and deconfinement of the breaking down of this symmetry. Also, an outline is given how to measure at different

temperatures.

In chapter 5 I show how the path integral expression for the thermal expectation value allows us to calculate in using Monte Carlo simulation. In a Markov simulation a Markov chain of gauge field configurations is generated. These are then used to calculate the thermal expectation value. All the preceding chapters are then combined in explaining how the script that I use works.

Finally, in chapter 6 results are shown for the order parameter. We will see that there are signs of a coexisting phase, which would be compatible with the claim that the phase transition is of order one.

Chapter 2

Expectation values: path integral formulation

In this chapter I introduce the crucial ingredients that precede gauge theory on a lattice. In chapter 4 we will see that we would like to calculate a the thermal expectation value $\langle P \rangle_{\beta_T}$, which measures the quark confinement.

The thermal expectation value of an observable O is given by

$$\langle O \rangle_{\beta_T} = \frac{1}{Z} \mathrm{tr} \left[e^{-\beta_T \hat{H}} \hat{O} \right], \tag{2.1}$$

where β_T is the inverse temperature, $\hat{H}$ the hamiltonian and $Z = \mathrm{tr} \left[e^{-\beta_T \hat{H}} \right]$.

The thermal expectation value Eq. 2.1 can be written in terms of path integrals. As we will see in chapter 5, this will allow us to calculate them using Monte Carlo simulation. To become familiar with several concepts and for simplicity we first consider the path integral formulation for scalar theory. Secondly, results are given for pure gauge theory, which will the starting point of analysis presented in this work.

2.1 Scalar theory

Path integral expressions for correlation functions for scalar theory are derived in many text books, e.g. [3]. As the approach for our *expectation values* is almost

analogues we will not give the full details of the derivation. Instead, in this section I give a summary of a derivation of the partition function $Z = \text{tr}\left[e^{-\beta\hat{H}}\right]$ for scalar theory with interaction terms $V(\phi)$, which can be found in [4]. This summary is meant to highlight a few conceptual issues. Our final expression will be a path integral with a discretised, so called, Euclidean action with fields ϕ which are periodic in the (Euclidean) time direction. As we will see the time and the space direction play different roles. The results for partition function is very easily generalised to expressions for $\text{tr}\left[e^{-\beta\hat{H}}O\right]$.

We consider a usual scalar theory with the Lagrangian $\mathcal{L} = \partial_\mu\phi\partial_\mu\phi - \frac{m^2}{2}\phi^2 - V(\phi)$, where $V(\phi)$ contains the interactions. The Hamiltonian for this system is

$$\hat{H} = \int d^3x \frac{1}{2}\hat{\pi}^2 + \frac{1}{2}\left(\nabla\hat{\phi}\right)^2 + V(\hat{\phi}), \tag{2.2}$$

where the fields $\hat{\phi}$ and its conjugate momentum $\hat{\pi}$ are operators that only depend on $\vec{x}$. This is the Hamilton we use to find an expression for $\text{tr}\left[e^{-\beta\hat{H}}\right]$.

At this stage we *regularise* the theory: we *discretise the Hamiltonian* by considering a finite volume $V = L^3$ and putting it on a lattice Λ_3 with N^3 points, where $\boxed{L = Na}$, for some lattice spacing a. The spacial coordinates are then given by $\vec{x} = a\vec{n}$ or simply $\vec{n}$. This approach leads more straight forwardly to the formulation of the path integral on the lattice. Physically it corresponds to imposing a *momentum cutoff* $\Lambda_{QCD} \sim \frac{1}{a}$. Concretely we replace

$$\int d^3x \to a^3 \sum_{\vec{n}\in\Lambda_3}, \tag{2.3}$$

$$(\nabla\phi)^2 \to \sum_{i=1}^{3}\left(\frac{\phi(\vec{n}+\hat{i}) - \phi(\vec{n}-\hat{i})}{2a}\right)^2, \tag{2.4}$$

and impose *periodic boundary conditions*: $\phi(\vec{n}) = \phi(\vec{n}+N\hat{i})$. The periodic boundary conditions only influence the notion of the derivatives at the boundaries. Note the periodic boundary conditions here are only an artifact from the discretisation.

Next, the main ingredient is to replace $e^{-\beta\hat{H}}$ by $(e^{-\epsilon\hat{H}})^N$, where $\boxed{\beta_T = \epsilon N_t}$. Then

$$Z = \text{tr}\left[e^{-\beta\hat{H}}\right] = \int d\phi_0 \left\langle\phi_0\right| \left(e^{-\epsilon\hat{H}}\right)^N \left|\phi_0\right\rangle, \tag{2.5}$$

where $|\phi_0\rangle$ are the eigenstates of the field operator $\hat{\phi}(\vec{n})$, i.e. $\hat{\phi}(\vec{n})\,|\phi_0\rangle = \phi_0(\vec{n})\,|\phi_0\rangle$.

Now, as usual, we insert identity $\mathbf{1} = \int d\phi_i\,|\phi_i\rangle\,\langle\phi_i|$ and similar expressions for $|\pi\rangle$. Then each of the inserted $|\phi_i\rangle$ represents a step in the Euclidean(!) time t, i.e $e^{-\epsilon\hat{H}}$ governs the "time evolution". Here is where we add this to the Euclidean time step as an argument of the field so that

$$\phi_i(\vec{n}) \equiv \phi(\vec{n}, i) \equiv \phi(\mathbf{n}), \tag{2.6}$$

so that $t = \epsilon n_4$. I would like to stress that the Euclidean time carries no particular physical interpretation, but it is only called time because of its mathematical similarities with the usual time.

The final expression for Z is, up to a proportionality factor which will drop out later,

$$Z = \int \mathcal{D}[\phi] e^{-S_E[\phi]}, \tag{2.7}$$

where in this derivation $S_E[\phi]$ is the discretised so called Euclidean action

$$S_E[\phi] = \epsilon a^3 \sum_{n\in\Lambda} \frac{1}{2}\left(\frac{\phi(\vec{n}, n_4+1) - \phi(\vec{n}, n_4)}{\epsilon}\right)^2 + \frac{1}{2}\sum_{i=1}^{3}\left(\frac{\phi(\vec{n}+\hat{i}, n_4) - \phi(\vec{n}-\hat{i}, n_4)}{2a}\right)^2 + V(\phi(\vec{n}, n_4)), \tag{2.8}$$

where, crucially, field ϕ is *periodic in the time direction*, i.e. $\phi(\vec{n}, N) = \phi(\vec{n}, 0)$ as a result of taking the trace in Eq. 2.5. The points n are taken in Λ, the $N^3 \times N_t$ space time lattice. Remember that $\beta_T = \epsilon N_t$ and $L = aN$. The measure is the product of the $d\phi$'s over all the points

$$\mathcal{D}(\phi) = \prod_{\mathbf{n}\in\Lambda} d\phi(\mathbf{n}). \tag{2.9}$$

To sum up, in principle discretised space and (Euclidean) time emerge and are treated separately. Their periodic boundary conditions are respectively a tool for convenience and a result of taking the trace. However, it is common to use set $\epsilon = a$ (so $\beta_T = aN_t$) and to replace $\frac{\phi(\vec{n},n_4+1)-\phi(\vec{n})}{\epsilon}$ by $\frac{\phi(\vec{n},n_4+1)-\phi(\vec{n},n_4-1)}{2\epsilon}$, so that space and time are treated the same. Then Eq. 2.8 can be seen as the

discretisation of

$$S_E[\phi] = \int_0^{\beta_T} dt \int d^3x \partial_\mu \phi \partial_\mu \phi + \frac{m^2}{2}\phi^2 + V(\phi), \tag{2.10}$$

where again $\phi(\vec{n}, 0) = \phi(\vec{n}, \beta_T)$ and the summation over μ is via a kronecker delta, rather than the Minkovski metric. This is why it is referred to as "Euclidean action". In section the next section we give the result for the Euclidean action for the gauge fields and in 3 we discretise it on the lattice.

A path integral expression for $\mathrm{tr}\left[e^{-\beta_T \hat{H}}\hat{O}\right]$ can be easily derived, for observables which are products of fields ϕ. Again we insert identities, which results in replacing the observable operators by their value at their given Euclidean time. We end up with

$$\langle O \rangle_{\beta_T} = \frac{1}{Z}\int \mathcal{D}[\phi] e^{-S_{E,\beta_T}[\phi]} O[\phi(\vec{x}, 0)], \tag{2.11}$$

where $Z = \int \mathcal{D}[\phi] e^{-S_E[\phi]}$, for $A = \beta_T, T$, defined as in Eqs. 2.7, 2.9 and 2.8. Note that here the proportionality factor drops out.

2.2 Pure gauge theory

This section is only meant to give results for pure gauge theory and I refer to [5] for further details and discussion. These results are very important, as they are the starting point for our analysis.

The Lagrangian for quantum chromodynamics (QCD) is given by

$$\mathcal{L}_{QCD} = -\frac{1}{2g^2}\mathrm{tr}\left[F_{\mu\nu}F^{\mu\nu}\right] + \sum_{i=1}^{N_f} \bar{\psi}_i (i\not{D} - m_i)\psi_i. \tag{2.12}$$

Here $F^a_{\mu\nu}$ is the $SU(3)$ field strength $iF_{\mu\nu} = [D_\mu, D_\nu]$ with $D_\mu = \partial + iA_\mu$ and $A_\mu = A^a_\mu T^a$ the Lie algebra valued gauge fields. Note that usually we formulate the Yang Mills action with gA_μ is the covariant derivative. The factor g^2 in front of $\mathrm{tr}\left[F_{\mu\nu}F^{\mu\nu}\right]$ compensates for this difference in definition. In chapter 3 it will become clear that the convention for the covariant derivative here is convenient in the formulation of the gauge action. As for the fermions, N_f is the number of

flavours, ψ_i represent quarks and $\not{D}$ is the covariant derivative contracted with gamma matrices. I use Lie algebra generators such that $\text{tr}\left[T^a T^b\right] = \frac{1}{2}\delta_{ab}$.

In the analysis of this work, we consider only pure gauge theory, i.e. the first term in the Lagrangian. Now in the derivation for the path integral, there are issues when taking the trace, as one should only include physical states [5]. However, it turns out that after a careful treatment using a projector operator (which is not discussion in the scope of this work), one arrives at the simple expression for the path integral:

$$Z_{\beta_T} = \int \mathcal{D}[A_\mu] e^{-S_G[A]} \tag{2.13}$$

where

$$\boxed{S_G[A] = \frac{1}{2g^2}\int_0^{\beta_T} dt \int d^3x \text{tr}\left[F_{\mu\nu}F_{\mu\nu}\right]}. \tag{2.14}$$

Again the gauge fields A_μ have to obey periodic boundary conditions $A_\mu(\mathbf{x}, \beta_T) = A_\mu(\mathbf{x}, 0)$.

Finally the expressions for the expectation values Eqs. 2.1 and **??**, in pure gauge theory are given by

$$\langle O \rangle_{\beta_T} = \frac{1}{Z}\int \mathcal{D}[A] e^{-S_G[A]} O[A(\vec{x}, 0)]. \tag{2.15}$$

In chapter 3 we will see how to represent the gauge fields and discretise $S_G[A]$ on the lattice. This will be helpful in defining $\langle P \rangle_{\beta_T}$, which measures the confinement.

Chapter 3

Discretised gauge action

Gauge groups ($SU(3)$ in our case) give rise to gauge fields. We introduce gauge fields in a slightly different fashion than usually. Our approach will be more geometrical and natural in the context of gauge fields to the lattice. Eventually we will see that gauge fields are represented by so called "link variables", elements of the gauge group. We then discretise the action in Eq. 2.14 in terms of these link variables. The tools and insights that we develop in this chapter will be very helpful in defining $\langle P \rangle_{\beta_T}$ in the next chapter.

3.1 Gauge fields revisited

In this section we introduce the *parallel transporter*, which allows to compare two vectors at different points on the manifold and thus to define the covariant derivative. The usual results for gauge fields A_μ, e.g. how they transform under gauge transformations, can be understood from the parallel transporter. It will become clear that it is a natural object on the lattice, because of finite distances between lattice points. The discussion of gauge fields follows roughly the same line as the one in chapter 4 of [6].

We consider n scalar fields $\Phi = (\Phi_1, \ldots, \Phi_n)$ on a manifold $\mathcal{M}$ transforming under an n-dimensional faithful representation of our gauge group G. One way to express this is follows. We associate to each point x on the manifold an n-dimensional vector space V_x. Then Φ picks a value in V_x at every point x, i.e. a

vector. Acting with G amounts to perform a linear transformation at each point of the form

$$\gamma(x) : V_x \to V_x, \tag{3.1}$$

such that $\Phi(x) \to \Phi'(x) = \gamma(x)\Phi(x)$.

Now we want to be able to compare two vectors at different point x and y on the manifold, so that we can take derivatives. We postulate that this is done by parallel transport along a curve $\mathcal{C}$ (from y to x: $\mathcal{C}(0) = y$, $\mathcal{C}(1) = x$) of a vector in V_y to a vector in V_x, using an object called the *parallel transporter*

$$\Gamma_{\mathcal{C}}(x, y) : V_y \to V_x, \tag{3.2}$$

whose matrix is an element of the gauge group. Note that $\Gamma_{\mathcal{C}}$ depends on the choice of $\mathcal{C}$

An important requirement is that our parallel transporter is *compatible* with gauge transformations. By this we mean that parallel transporting first and then do the gauge transformation, should give the same results as performing a gauge transformation first and take the (gauge transformed) parallel transportation:

$$\gamma(x)\Gamma_{\mathcal{C}}(x, y)\Phi(y) = \Gamma'_{\mathcal{C}}(x, y)\gamma(y)\Phi(y). \tag{3.3}$$

Note that on the LHS we indeed parallely transport $\Phi(y)$ to x and then do the gauge transformation at point x, whereas on the right hand side we gauge transform at y before we gauge-transformed-parallely transport to x. This is requirement can be conveniently written as

$$\boxed{\Gamma'_{\mathcal{C}}(x, y) = \gamma(x)\Gamma_{\mathcal{C}}(x, y)\gamma^{-1}(y)}. \tag{3.4}$$

In the next section we will consider infinitesimal parallel transport. This will allow us to introduce our usual gauge fields with their transformation law. Also we derive the expression for the covariant derivative.

3.1.1 Infinitesimal parallel transport: gauge fields and covariant derivative

Let us introduce some notation. We parametrise the curve $\mathcal{C}$ with $z : [0,1] \to \mathcal{M}$, so that $y = z(0)$ and $x = z(1)$. We denote $\Phi(s)$ the field $\Phi(y)$ parallely transported along $\mathcal{C}$ to point $z(s)$:

$$\Phi(s) = \Gamma_{\mathcal{C}}(z(s), y)\Phi(y). \tag{3.5}$$

Now we consider and infinitesimal transportation $\Phi(s+\epsilon)$:

$$\begin{aligned}\Phi(s+\epsilon) &= \Gamma_{\mathcal{C}}(z(s+\epsilon), z(s))\Phi(s) \\ &= \left[\mathbf{1} + \epsilon\dot{z}^{\mu}(s)\frac{\partial\Gamma_{\mathcal{C}}(z', z(s))}{\partial z'^{\mu}}\right]\Phi(s) \\ &\equiv \left[\mathbf{1} - i\epsilon\dot{z}^{\mu}A_{\mu}(z(s))\right]\Phi(s),\end{aligned} \tag{3.6}$$

where we have *introduced the gauge field* A_μ. Note that $\Gamma_{\mathcal{C}}(z(s+\epsilon), z(s))$ is an element of G, so that A_μ is Lie algebra valued.

For reference we note that we have found the differential equation relating our parallel transporter to the gauge field:

$$\frac{\mathrm{d}\Gamma_{\mathcal{C}}(z(s'), z)}{\mathrm{d}s'} = -i\dot{z}^{\mu}A_{\mu}(z), \tag{3.7}$$

where we denote $z = z(s)$. This expression is solved using a path ordered exponential as we will see later.

We can now deduce the transformation law for the gauge fields using our requirement for the transformation of the parallel transporter (Eq. 3.4) and Eq. 3.6:

$$\begin{aligned}\mathbf{1} - i\epsilon\dot{z}\cdot A' &= \gamma(z(s+\epsilon))\left[\mathbf{1} - i\epsilon\dot{z}\cdot A\right]\gamma^{-1}(z) \\ &= \mathbf{1} - i\epsilon\dot{z}^{\mu}\left[\gamma(z)A_{\mu}\gamma^{-1}(z) + i\partial_{\mu}\gamma(z)\gamma(z)\right],\end{aligned} \tag{3.8}$$

where we have suppressed the argument $z(s)$ for A, A' and $\dot{z}$. We indeed find the

usual *transformation law* for the gauge fields:

$$\boxed{A'_\mu = \gamma A_\mu \gamma^{-1} + i\left(\partial_\mu \gamma\right)\gamma^{-1}.} \tag{3.9}$$

We can now understand the notion of the covariant derivative. Consider again an infinitesimal curve, starting at z. We take the limit of subtracting Φ, parallelly transported to $z(s+\epsilon)$, from Φ at that point:

$$\begin{aligned} &\lim_{\epsilon\to 0} \frac{\Phi(z(s+\epsilon)) - \Gamma_{\mathcal{C}}(Z(s+\epsilon), z)\Phi(z)}{\epsilon} \\ =&\lim_{\epsilon\to 0} \frac{\Phi + \epsilon \dot{z}\cdot\partial\Phi - \left[\mathbf{1} - \epsilon i \dot{z}\cdot A\right]\Phi + \mathcal{O}(\epsilon^2)}{\epsilon} \\ =&\dot{z}\cdot\left[\partial + iA\right]\Phi \equiv \dot{z}\cdot D\Phi \end{aligned} \tag{3.10}$$

Again we see that we get the familiar expression for the *covariant derivative*

$$\boxed{D = \partial + iA.} \tag{3.11}$$

Note that for a vector field along a curve which is the result of the parallel transport of a vector along that curve, the covariant derivative along this curve equals zero.

Let us now come back to the the differential Eq. 3.7. Note that this is similar to the general Schrödinger equation, where the Hamiltonian $\hat{H}$ is allowed to be time dependent. We can solve this by a so called "path ordered integral" given by

$$\Gamma_{\mathcal{C}}(x,y) = P\exp\left(-i\int_{\mathcal{C}} ds \dot{z}\cdot A\right). \tag{3.12}$$

To see that this expression satisfies our constraint, Eq. 3.4, let us write Eq. 3.12 as the limit of N infinitesimal gauge transformations:

$$\Gamma_{\mathcal{C}}(x,y) = \lim_{N\to\infty}\left[\mathbf{1} - \frac{i}{N}\dot{z}\left(\frac{N-1}{N}\right)\cdot A\right]\ldots\left[\mathbf{1} - \frac{i}{N}\dot{z}(0)\cdot A\right]. \tag{3.13}$$

A gauge transformation would then yield

$$\Gamma'_{\mathcal{C}}(x,y) = \gamma(x)[\ldots]\gamma^{-1}\left(z\left(\frac{N-1}{N}\right)\right)\gamma\left(z\left(\frac{N-1}{N}\right)\right)\cdots\gamma\left(z\left(\frac{1}{N}\right)\right)[\ldots]\gamma^{-1}(y), \tag{3.14}$$

which gives us indeed the right transformation law under gauge transformation.

For reference we state that another obvious property of the parallel transporter is that they can be composed

$$\Gamma_{\mathcal{C}_1}(x,z)\Gamma_{\mathcal{C}_2}(z,y) = \Gamma_{\mathcal{C}}(x,y), \tag{3.15}$$

where $\mathcal{C}$ is the path composed of $\mathcal{C}_1$ and $\mathcal{C}_1$.

3.2 Gauge fields on the lattice

We now have the ingredients to construct the discretised action for the gauge fields on a lattice. First we need to define a lattice and represent the gauge fields, as we will see, by link variables. Using the link variables we write down the Wilson action and check that it resembles the continuum action, from Eq. 2.14.

Consider a 4-dimensional hyper cubic lattice, with spacing a. The fourth direction represents the *Euclidean time*. We can assign labels n_μ or simply n to the sites, corresponding to Euclidean coordinates $x_\mu = an_\mu$. Now, how do we represent a gauge field on the lattice? Note that the sites are discrete points in space time. Remember that the usual gauge field A_μ came about by considering parallel transport along an infinitesimal curve. This suggests that in our discrete case we need to consider parallel transporters on the links between lattice sites. It turns out to have a notational advantage to define the *link variable* on the link connecting site $n + \hat{\mu}$ with n:

$$\Gamma(n, n+\hat{\mu}) \equiv U_\mu(n) = \exp(iaA_\mu(n)). \tag{3.16}$$

Indeed, assuming A_μ to be approximately constant along the link, i.e $A(n) \approx A(n+\hat{\mu})$, this is the path ordered integral, defined in Eq. 3.12. Using Eq. 3.4 it can readily be seen that under a gauge transformation $U_\mu(n)$ transforms as

$$U_\mu(n) \to \gamma(n)U_\mu(n)\gamma^{-1}(n+\hat{\mu}). \tag{3.17}$$

Further note that from the definition Eq. 3.16 we have that

$$U_{-\mu}(n+\hat{\mu}) = U_{\mu}^{\dagger}(n). \tag{3.18}$$

Now before defining the lattice action, let us first introduce a pictorial way of viewing the link variables.

3.2.1 Visualisation

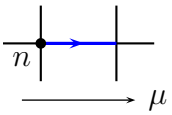

Figure 3.1: The blue line represents $U_{\mu}(n)$, the link variable starting at n pointing in the μ direction.

It turns out that our link variables $U_{\mu}(n)$ can be conveniently depicted as a directed line, i.e with an arrow, starting at n, going in the μ direction, see Fig. 3.1. I want to point out here that although $U_{\mu}(n)$ is the parallel transporter from $n+\hat{\mu}$ to n, Fig. 3.1 and the notation $U_{\mu}(n)$ suggest parallel transport"from n to $n+\hat{\mu}$. This may seem confusing, but it has a notational advantage in the translation of parallel transport on the lattice, as is pointed out below.

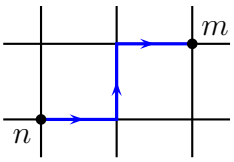

Figure 3.2: A Wilson line is a sequence of connected lines. It corresponds to parallel transporter from m to n (not a typo!), c.f. Eq. 3.12.

We define a *Wilson line* as a sequence of connected link variables, see Fig. 3.2. This is the lattice equivalent of the parallel transporter (Eq. 3.12) from the *end* to the *starting* point in terms of link variables along the line. The path ordered integral amounts to taking the *right product* of the matrices corresponding to the

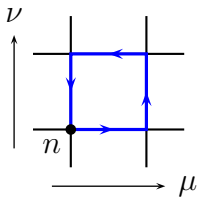

Figure 3.3: The plaquette $U_{\mu\nu}$ is the closed Wilson line, starting at n which goes in the μ-, then in the ν-direction and back.

links

$$\prod_{l\in\mathcal{L}} U_l = U_1 \cdots U_N, \tag{3.19}$$

where l stands for the μ and n labels along the line $\mathcal{L}$. We will consider various closed Wilson lines: the Plaquette and the Polyakov loop in respectively the next section and chapter 4.

3.3 Eucledian action

We now have all the tools to discretise Euclidean action Eq. 2.14 for the gauge fields. We start of by defining the simplest closed Wilson line, the *plaquette* $U_{\mu\nu}$, starting a point n first going in the μ- and then in the ν-direction and back

$$U_{\mu\nu}(n) = U_\mu(n)U_\nu(n+\hat{\mu})U_\mu^\dagger(n+\hat{\nu})U_\nu^\dagger(n). \tag{3.20}$$

See also Fig. 3.3. Note that under a gauge transformation $U_{\mu\nu}(n) \to \gamma(n)U_{\mu\nu}\gamma_{-1}(n)$ the trace of $U_{\mu\nu}(n)$ is thus gauge invariant.

The *Wilson gauge action* is defined as [7]:

$$\boxed{S_G[U] = \frac{\beta}{3}\sum_{n\in\Lambda}\sum_{\mu<\nu}\text{Re tr}\left[\mathbf{1} - U_{\mu\nu}(n)\right].}, \tag{3.21}$$

where $\beta = \frac{b}{g^2}$, Λ is our $N^3 \times N_t$ lattice with lattice spacing a, such that $L = aN$ and $\beta_T = aN_t$. Note that β is subjected to conventions for $\text{tr}\,[T_aT_b]$ of the generators, but the form of the Wilson action does not change. Also, β should not be confused with the inverse temperature β_T.

We can calculate $U_{\mu\nu}(n)$ using the BKH formula $\exp(A)\exp(B) = \exp(A +$

$B + \frac{1}{2}[A, B] + \ldots$). If we denote $A = aA_\mu(n)$, $B = aA_\nu(n + \hat{\mu})$, $C = aA_\mu(n + \hat{\nu})$ and $D = aA_\nu(n)$, then to order a^3 we find

$$\begin{aligned} U_{\mu\nu}(n) &= e^{iA}e^{iB}e^{-iC}e^{-iD} = e^{i(A+B)-\frac{1}{2}[A,B]+\mathcal{O}(a^3)}e^{-i(C+D)-\frac{1}{2}[C,D]+\mathcal{O}(a^3)} \\ &= e^{i(B-D)-i(C-A)+\frac{1}{2}([A,C]+[A,D]+[B,C]+[B,D]-[A,B]-[C,D])+\mathcal{O}(a^3)}. \end{aligned} \tag{3.22}$$

We note that we can write $A_\mu(n + \hat{\nu}) = A_\mu(n) + a\partial_\nu A_\mu(n)$ and $A_\nu(n + \hat{\mu}) = A_\nu(n) + a\partial_\mu A_\nu(n)$. Then it is easy to verify that

$$\begin{aligned} U_{\mu\nu}(n) =& e^{ia^2(\partial_\mu A_\nu(n)-\partial_\nu A_\mu(n)+i[A_\mu(n),A_\nu(n)])+\mathcal{O}(a^3)} \\ =& e^{ia^2 F_{\mu\nu}(n)+\mathcal{O}(a^3)}. \end{aligned} \tag{3.23}$$

Now expanding this expression yields

$$U_{\mu\nu}(n) = \ + \left[ia^2 F_{\mu\nu}(n) + \mathcal{O}(a^3)\right] - \left[\frac{a^2}{2}F_{\mu\nu}(n)F_{\mu\nu}(n) + \mathcal{O}(a^6)\right]. \tag{3.24}$$

Plugging this into Eq. 3.21, the identities cancel and the linear term, which is Lie algebra valued, is killed by the trace. Since $tr(U_{\mu\nu}(n))^* = tr(U_{\mu\nu}(n)^\dagger) = tr(U_{\nu\mu})$ and $F_{\mu\nu}$ is antisymmetric, taking the real part amounts to replacing 2Re $\sum_{\mu<\nu}$ by $\sum_{\mu,\nu}$, so that

$$S_G[U] = \frac{a^4}{2g^2}\sum_n \sum tr\left[F_{\mu\nu}(n)^2\right] + \mathcal{O}(a^6), \tag{3.25}$$

where the summation over μ and ν is now implicit. We see that indeed this expression resembles Eq. 2.14.

In conclusion, we have seen how gauge fields should be represented on the lattice. We also discretised the gauge action 2.14, needed to calculate thermal expectation values using 2.15. In the next chapter we introduce an order parameter, which measures confinement of a single quark. It will turn out that it can be written like the thermal expectation value of the Polyakov loop $\langle P\rangle_{\beta_T}$, such that we can use the tools developed thus far. The rest of the work will then be devoted to calculating this quantity numerically.

Chapter 4

Quark confinement

The aim of this work is to investigate confinement of a single quark at finite temperature. In this chapter I introduce an order parameter, which measures this confinement. It turns out that this order parameter is a thermal expectation value $\langle P \rangle_{\beta_T}$ which allows us to calculate it on the lattice, see chapter 6. We will see how (de)confinement can be understood in terms of the (breaking of) Z_3 symmetry. Finally I will point out how we can vary the temperature.

4.1 Order parameter

In this section I give the definition of an order parameter [2] based on $F_{N_q N_{\bar{q}}}$the free energy of N_q heavy, static quarks $\psi_a(\vec{r_i}, t)$ and $N_{\bar{q}}$ anti quarks $\psi_b^c(\vec{r_j}, t)$.

We admit [2] that the *free energy* $F_{N_q N_{\bar{q}}}$ is defined by

$$e^{-\beta F_{N_q N_{\bar{q}}}} = \frac{1}{N^{N_q + N_{\bar{q}}}} \sum_{|s\rangle} \langle s | \, e^{-\beta \hat{H}} \, | s \rangle \,, \tag{4.1}$$

where $N_c = 3$ in our case of $SU(3)$, $|s\rangle$ are states with N_q ($N_{\bar{q}}$) *heavy, static* (anti) quarks at positions $r_1 \dots r_{N_q}$ ($r'_1 \dots r'_{N_{\bar{q}}}$). Defining $e^{-\beta \Delta F_{N_q N_{\bar{q}}}} \equiv \frac{e^{-\beta F_{N_q N_{\bar{q}}}}}{e^{-\beta F_{00}}}$, we derive in section 4.1.1 that

$$e^{-\beta \Delta F_{N_q N_{\bar{q}}}} = \langle P^\dagger(\vec{r}_1) \cdots P^\dagger(\vec{r}_{N_q}) P(\vec{r'}_1) \cdots P(\vec{r'}_{N_{\bar{q}}}) \rangle_{\beta_T}, \tag{4.2}$$

the thermal expectation value, see Eq. 2.15, of Polyakov loops (in the literature

also often called Wilson line L)

$$P(\vec{r}) = \frac{1}{N_c}\text{tr}\left[P\exp i\int_0^\beta dtA_4(\vec{r},t)\right], \tag{4.3}$$

for which we can give a discretised expression in terms of link variables

$$P(\vec{r}) = \frac{1}{N_c}\text{tr}\left[\prod_{i=0}^{N-1} U_4(\vec{r},i)\right]. \tag{4.4}$$

Note that remarkably Eq. 4.2 is fully expressed in terms of only gauge fields.

We now define the *order parameter* as using the free energy of one quark

$$\boxed{e^{-\Delta F_{10}} = \langle P\rangle_{\beta_T},} \tag{4.5}$$

where the Polyakov loop P is calculated for some point $\mathbf{m}$. (De)Confinement of the quark is defined as

$$\begin{aligned}\langle P\rangle_{\beta_T} &= 0 \text{ confinement}\\ \langle P\rangle_{\beta_T} &\neq 0 \text{ deconfinement.}\end{aligned} \tag{4.6}$$

or equivalently having a divergent (finite) free energy. We can interpret $\langle P\rangle_{\beta_T}$ in terms of centre symmetry, as we will see in section 4.2. It turns out that deconfinement corresponds to breaking of the symmetry and gives $\langle P\rangle_{\beta_T} = zP_0$, with $z = 1, e^{\pm\frac{2\pi i}{3}}$.

4.1.1 Derivation

In this section I derive the result Eq. 4.2. This derivation follows the one given in [2], but I highlight some physical assumptions.

We consider N_q heavy, static quarks $\psi_a(\vec{r_i},t)$ and $N_{\bar{q}}$ anti quarks $\psi_b^c(\vec{r_j},t)$. The anti quarks are charge conjugates of quarks. Their positions are given by r_i for the quarks and r'_j for the anti quarks. Quarks transform under $SU(3)$ in the fundamental- , anti quarks in the anti fundamental representation and the labels a and b denote the colour indices.

We will need quark- and anti quark- equal time anti commutation relations

(ETAR). The quarks obey

$$\left\{\psi_a(\vec{r}_i,t),\psi_b^\dagger(\vec{r_j},t)\right\}=\delta_{ij}\delta_{ab}, \tag{4.7}$$

whereas all others quark ETAR vanish, as well as ETAR between quarks and antiquarks. The ETAR for the anti quarks are analogous to the quarks.

Now, considering very heavy quarks yields an effective action [8]

$$S_{HQ}=\int dt\bar{\psi}(\vec{x},t)\frac{1}{i}\gamma^0D^0\psi(\vec{x},t) \tag{4.8}$$

such that classical equations of motion give that the covariant derivative in the time direction vanishes

$$\left(\frac{\partial}{\partial t}+iA_4(\vec{r},t)\right)\psi(\vec{r},t)=0, \tag{4.9}$$

i.e. the time evolution of the quark is governed by its parallel transport along the curve connecting $(\vec{r},0)$ and $(\vec{r},t)$, so that at time t we have

$$\psi(\vec{r},t)=\Gamma\left((\vec{r},t),(\vec{r},0)\right)\psi(\vec{r},0)=T\exp\left(-i\int dtA_4(t)\right)\psi(\vec{r},0). \tag{4.10}$$

Note that anti quarks transform in the anti fundamental representation, such that $-iA_4$ gets replaced by iA_4.

An important assumption is that the operators ψ, evolving by Euclidean time evolution,

$$\psi(\vec{r},t)=e^{\beta\hat{H}}\psi(\vec{r},o)e^{-\beta\hat{H}}. \tag{4.11}$$

also follow Eq. 4.10.

Now consider Eq. 4.1. Using the quark and anti quark creation operators we can write

$$\sum_{|s\rangle}|s\rangle=\sum_{|s'\rangle}\sum_{\{a,b\}}\psi_{a_1}^\dagger(\vec{r}_1,0)\cdots\psi_{a_{N_q}}^\dagger(\vec{r}_{N_q},0)\psi_{b_1}^{c\dagger}(\vec{r}_1,0)\cdots\psi_{b_{N_{\bar{q}}}}^{c\dagger}(\vec{r}_{N_{\bar{q}}},0)\left|s'\right\rangle, \tag{4.12}$$

where $|s'\rangle$ are states with no heavy quarks. Then Eq. 4.1 gives

$$e^{-\beta F_{N_q N_{\bar{q}}}} = \frac{1}{N_c^{N_q+N_{\bar{q}}}} \sum_{|s'\rangle} \sum_{\{a,b\}} \langle s'| \psi^c_{b_{N_{\bar{q}}}}(\vec{r}_{N_{\bar{q}}}, 0) \dots \psi^c_{b_1}(\vec{r}_1, 0) \psi_{a_{N_q}}(\vec{r}_{N_q}, 0) \dots \psi_{a_1}(\vec{r}_1, 0) e^{-\beta \hat{H}} \\ \times \psi^\dagger_{a_1}(\vec{r}_1, 0) \cdots \psi^\dagger_{a_{N_q}}(\vec{r}_{N_q}, 0) \psi^{c\dagger}_{b_1}(\vec{r}_1, 0) \cdots \psi^{c\dagger}_{b_{N_{\bar{q}}}}(\vec{r}_{N_{\bar{q}}}, 0) |s'\rangle \tag{4.13}$$

Now we insert identities $\mathbf{1} = e^{-\beta \hat{H}} e^{\beta \hat{H}}$ left of the ψ and ψ^c. Using the expression for the Euclidean time evolution, Eq. 4.11, and the ETAR, Eq. 4.7, we find that

$$e^{-\beta F_{N_q N_{\bar{q}}}} = \frac{1}{N_c^{N_q+N_{\bar{q}}}} \sum_{|s'\rangle} \sum_{\{a,b\}} \langle s'| e^{-\beta \hat{H}} \psi_{a_1}(\vec{r}_1, \beta) \psi^\dagger_{a_1}(\vec{r}_1, 0) \cdots \psi_{a_{N_q}}(\vec{r}_{N_q}, \beta) \psi^\dagger_{a_{N_q}}(\vec{r}_{N_q}, 0) \\ \times \psi^c_{b_1}(\vec{r}_1, \beta) \psi^{c\dagger}_{b_1}(\vec{r}_1, 0) \cdots \psi^c_{b_{N_{\bar{q}}}}(\vec{r}_{N_{\bar{q}}}, \beta) \psi^{c\dagger}_{b_{N_{\bar{q}}}}(\vec{r}_{N_{\bar{q}}}, 0) |s'\rangle \,. \tag{4.14}$$

The next step is where the magic happens and where we get rid of the quarks. Now note that e.g.

$$\begin{aligned} \psi^c_{b_{N_{\bar{q}}}}(\vec{r}_{N_{\bar{q}}}, \beta) \psi^{c\dagger}_{b_{N_{\bar{q}}}}(\vec{r}_{N_{\bar{q}}}, 0) |s'\rangle &= \Gamma\left((\vec{r}_{N_{\bar{q}}}, \beta), (\vec{r}_{N_{\bar{q}}}, 0)\right)_{b_{N_{\bar{q}}} b} \psi^c_b(\vec{r}_{N_{\bar{q}}}, 0) \psi^{c\dagger}_{b_{N_{\bar{q}}}}(\vec{r}_{N_{\bar{q}}}, 0) |s'\rangle \\ &= \Gamma\left((\vec{r}_{N_{\bar{q}}}, \beta), (\vec{r}_{N_{\bar{q}}}, 0)\right)_{b_{N_{\bar{q}}} b} \left(\delta_{b N_{\bar{q}}} - \psi^{c\dagger}_{b_{N_{\bar{q}}}}(\vec{r}_{N_{\bar{q}}}, 0) \psi^c_b(\vec{r}_{N_{\bar{q}}}, 0)\right) |s'\rangle \\ &= \mathrm{tr}\left[T \exp\left(+i \int dt A_4(t)\right)\right] |s'\rangle \,, \end{aligned} \tag{4.15}$$

where we have used the ETAR, Eq. 4.7 in the first step and the fact that ψ annihilates a state with no quarks. Repeating this process and using Eq. 4.3 yields

$$e^{-\beta F_{N_q N_{\bar{q}}}} = \sum_{|s'\rangle} \langle s'| e^{-\beta \hat{H}} P^\dagger(\vec{r}_1) \cdots P^\dagger(\vec{r}_{N_q}) P(\vec{r'}_1) \cdots P(\vec{r'}_{N_{\bar{q}}}) |s'\rangle \,, \tag{4.16}$$

which is equal to the trace over only the gauge fields. If we now divide by $e^{-F_{00}}$, we arrive at the desired equation Eq. 4.2

4.2 Centre symmetry

As announced, we can understand deconfinement from Z_3 symmetry breaking, which I explain in this section.

Let us consider gauge transformations $U_\mu(n) \to \gamma(n)U_\mu(n)\gamma^{-1}(n+\hat{\mu})$. Remember that we have periodic boundary conditions for the link variables in the time $U_\mu((m),\beta) = U_\mu(\mathbf{m},0)$. Gauge transformations have to preserve this. We admit that a *necessary* [5] condition is

$$\gamma(\mathbf{m},N_t) = C\gamma(\mathbf{m},0), \tag{4.17}$$

where $C \in Z_3$ the centre of $SU(3)$. The centre is the subgroup that commutes with all other elements and in the case of $SU(3)$ it is $Z_3 = \left\{z\mathbf{1},\ \text{with } z = 1, e^{\frac{2\pi i}{3}}, e^{\frac{-2\pi i}{3}}\right\}$. We see that indeed

$$U_\mu(\mathbf{m},N_t) \to U'_\mu(\mathbf{m},N_t) = C\gamma(\mathbf{m},N_t)U_\mu(n)\gamma^{-1}\left((\mathbf{m},1)+\hat{\mu}\right)C^{-1} = U'_\mu(\mathbf{m},0), \tag{4.18}$$

where we have used the periodic boundary condition for γ and the fact that C commutes with all elements of $SU(3)$.

We note here that a gauge transformation with a periodic boundary condition as in 4.17 does not affect the action, Eq. 3.21. The only concern would be plaquettes which involve $U_4(\mathbf{m},N_t-1)$, but in these plaquettes the inverse appears as well, such that the contribution of C cancels.

The important point however is that the Polyakov loop P *does* change like $P \to zP$. So for the free energy we have

$$e^{-\beta\Delta F_{N_qN_{\bar{q}}}} \to z^{(N_q-N_{\bar{q}})}e^{-\beta\Delta F_{N_qN_{\bar{q}}}}, \tag{4.19}$$

which suggests that our order parameter vanishes if $N_q - N_{\bar{q}}$ is not a multiple of 3, which explains confinement. Our order parameter $\langle P\rangle_{\beta_T}$ thus vanishes as long as the centre symmetry is not broken. This is called the symmetric phase.

If our order parameter does not vanish, then the centre symmetry is broken and we expect find 3 states with corresponding $\langle P\rangle_{\beta_T} = zP_0$.

4.3 Varying the temperature

Given a certain lattice, the parameter that we can tune is the inverse coupling β in our action, Eq. 3.21. In the physical interpretation of the results we would

like to know how β relates to the temperature $T = \frac{1}{aN_t}$.

Note that our physical cutoff is defined by the lattice size a. Therefore we expect β to be running as a function of a. Doing complete injustice to the underlying physics, I simply quote the result form [9]:

$$a(\beta) = r_0 \exp\left(-1.6804 - 1.7331(\beta - 6) + 0.7849(\beta - 6)^2 - 0.4428(\beta - 6)^3\right) \quad \text{for } 5.7 \leq \beta \leq 6.92 \tag{4.20}$$

where $r_0 = 0.5\ fm$ is called the Sommer parameter, after Rainer Sommer who introduced it in [10]. Eq. 4.20 is based on extracting the static potential between two quarks calculated from *Wilson loops*, see e.g. [11].

The important information for us is that since a is a decreasing function of β, *the temperature* $T = \frac{1}{aN_t}$ *increases with* β. I will give the results of my simulation in terms of β and only use Eq. 4.20 to calculate the temperature of the phase transition.

In the next chapter I show how we can numerically calculate $\langle P \rangle_{\beta_T}$. I present my results in chapter 6.

Chapter 5

Monte Carlo simulation

As we have seen in the previous chapters, we want to calculate thermal expectation values the Polyakov loop P

$$\langle O \rangle_{\beta_T} = \frac{\mathrm{tr}\left[e^{-\beta \hat{H}} P\right]}{\mathrm{tr}\left[e^{-\beta \hat{H}}\right]} = \frac{1}{Z} \int \mathcal{D}[U] e^{-S_G[U]} P[U], \tag{5.1}$$

where $Z = \int \mathcal{D}[U] e^{-S_G[U]}$, $S_G[U]$ is the Euclidean action for the link variables (Eq. 3.21).

We will see that we can estimate the thermal expectation value of an observable $O[U]$ as the sum

$$\langle O \rangle_{\beta_T} = \frac{1}{N} \sum_{i=1}^{N} O[U_i], \tag{5.2}$$

where the summation is carried out over random *configurations* U_i. Crucial in this sum is to take the configurations U_i according to the Boltzmann distribution $\propto e^{-S_G[U_i]}$.

In this chapter I explain why a Markov chain provides us correctly distributed configurations and under which conditions. Then I introduce the Metropolis algorithm and show that it fulfils these conditions. Finally I describe how it is efficiently implemented in the program that I use [12], as to produce the sequence of configurations. This process is called a *Monte Carlo simulation*.

I should note here that sections 5.1 and 5.2 follow roughly the discussion given in chapter 4 of [4]. However, I do feel that they are necessary to understand the

understand the script that I use.

5.1 The idea

Imagine one would like to calculate the avarage of a function f over an interval $[a, b]$:

$$\langle f \rangle = \frac{1}{b-a} \int_a^b dx f(x). \tag{5.3}$$

One way of approximation this integral is to take N values $x_i \in [a, b]$ uniformly distributed and calculate the sum

$$\langle f \rangle \approx \lim_{N \to \infty} \frac{1}{N} \sum f(x_i). \tag{5.4}$$

Next we consider the expectation value of $f(x)$, again over the interval $[a, b]$, now with x randomly distributed according to a probability $\propto \rho(x)$, for some density function ρ:

$$\langle f \rangle = \frac{1}{Z} \int_a^b dx \rho(x) f(x), \text{ with } Z = \int_a^b dx \rho(x). \tag{5.5}$$

Note that this expression starts to look like Eq. 5.1. We can again estimate this expectation value as in Eq. 5.4, only now taking x_i randomly distributed according to

$$dP(x) = \frac{\rho(x) dx}{Z}. \tag{5.6}$$

Why is this useful to us? It is easy to see that expressions like Eq. 5.1 would involve enormous integrals. Consider for example a modest hyper cubic lattice with length 8 in 4 dimensions. Then the integral measure becomes

$$\mathcal{D}[U] = \prod_{n,\mu} dU_\mu(n), \tag{5.7}$$

so we would have to integrate over $8^4 \times 4 = 16384$ link variables. This would be a very cumbersome computation and it gets much worse as one goes to larger lattices. Therefore, in order to numerically compute the expectation value Eq. 5.1, we need expression Eq. 5.2.

Given *one* configuration U of link variables $U_\mu(n)$ on the lattice, it is easy to calculate the corresponding value of the observable. As we will see, the main challenge is to generate an ensemble of configurations U_i in accordance with the probability density $\propto e^{-S_G[U_i]}$.

5.2 Generating configurations

We have argued in the last section that in order to calculate the expectation value for the Wilson loop on a lattice, we need to generate configurations U_i of the link variables $U_\mu(n)$. These configurations must crucially be chosen according to a probability $e^{-S_G[U]}$.

We do this by creating a Markov chain, a random sequence of configurations U_i. In this section we will first review a little bit of theory about Markov chains, in particular *conditions* on the transition probability. Once we have understood this we will see how the widely used Metropolis algorithm fulfils these conditions. We will also see that the Metropolis algorithm is particularly useful in our case where the configurations scale with a Boltzmann factor. The ideas in this section are of vital importance to understand the script that I use (section 5.3) to generate the link variable configurations.

5.2.1 Markov Chains

The main ingredient for a Markov Chain is the transition probability T from one configuration U to another, say U'. In this section I will give the *defining property* and two important *constraints* for T.

Consider the configuration space, containing all configurations U of the link variables. We want to construct a Markov Chain: a sequence

$$U_0 \xrightarrow{T} U_1 \xrightarrow{T} \ldots \xrightarrow{T} U_N \tag{5.8}$$

of configurations, randomly "chosen" with a transition probability T. The defining property for T is that the probability to go from one configuration U_i to the

next U_{i+1} does not depend on i:

$$T(U_{i+1} = U'|U_i = U) = T(U'|U). \tag{5.9}$$

One reasonable constraint on T is that the probability to go from a configuration U to any other U' (including U itself), should be equal to 1:

$$\sum_{U'} T(U'|U) = 1. \tag{5.10}$$

A way of visualising this is taking a finite configuration space, with configurations $\mathbf{i} = (0, \ldots, 1, \ldots, 0)^T$. Then $T(\mathbf{j}|\mathbf{i})$ is a matrix and its collumns add up to one. In the following I will refer to this matrix for explanation sake, but one should keep in mind that we do in fact have an infinite configuration space.

Concretely the Markov process will go as follows. One starts of with a configuration U_0. The next configurations U_1 is randomly chosen according to $T(U_1|U_0)$. Repeating this process N times amount to applying our "matrix" N times. For stability to occur we would like to see that applying the matrix $N + 1$ for large N gives the same probability as applying the matrix N times:

$$T^{N+1}\mathbf{i} = T^N\mathbf{i}, \text{ or equivalently } T\mathbf{p} = \mathbf{p}, \tag{5.11}$$

where $\mathbf{p}$ is the equilibrium vector containing the probabilities to be in any of the configurations. The configurations in our sequence should be distributed in configuration space according to the probabilities in $\mathbf{p}$.

We need two important restrictions on the transition probability T to ensure that we end up in equilibrium. Firstly, we want that all configurations are accessable in a finite number of steps, i.e. $T^k(\mathbf{j}|\mathbf{i}) > 0$ for some k. This condition is called *ergodicity*.

Seconly, there should not be probability sinks or sources, loosely speaking "it should be as likely to visit as to leave a configuration". This means that the probability to be in U and to go to any next configuration U', must equal the

probability of coming to U from any former configuration U':

$$\sum_{U'} T(U'|U)P(U) = \sum_{U'} T(U|U')P(U'). \tag{5.12}$$

This is called the *balance condition*. We immediately see that this amounts to being in equilibrium, by carrying out the summation on the LHS. We find

$$\sum_{U'} T(U|U')P(U') = P(U), \tag{5.13}$$

which is indeed what one would expect in equilibrium, c.f. Eq. 5.11.

There is a somewhat stronger condition on T that ensures the balance condition Eq. 5.12, called the *detailed balance condition*

$$T(U'|U)P(U) = T(U|U')P(U') \tag{5.14}$$

We will see that Metropolis algorithm, which we will use, guarantees this condition.

5.2.2 Metropolis algorithm

We have seen that a Markov chain of configurations can be generated using a transition function. These configurations U_i will eventually be distributed like $e^{-S_G[U_i]}$ if the transition function obeys *ergodicity* and the *(detailed) balance condition*.

The Metropolis algorithm governs the transition from configuration U_{i-1} to U_i. Every transition consist of two steps:

- **Step 1:** Given the current configuration U a candidate configuration U' is chosen according to an *a priori* transition function T_0.
- **Step 2:** The candidate is accepted with probability $P_A = \min\left\{1, \frac{T_0(U|U')P(U')}{T_0(U'|U)P(U)}\right\}$. If the candidate is not accepted, the next configuration will remain U.

The total transition probability is is thus the product of the a priori transition function and the acceptance probability $T(U'|U) = P_A T_0(U'|U)$. This T obeys the

detailed balance condition, if $T_0(U'|U) > 0$ for all U and U' (strong ergodicity):

$$\begin{aligned} T(U'|U)P(U) =& T_0(U'|U)P(U)\min\left\{1, \frac{T_0(U|U')P(U')}{T_0(U'|U)P(U)}\right\} \\ =& \min\left\{T_0(U'|U)P(U), T_0(U|U')P(U')\right\} \\ =& T(U|U')P(U'). \end{aligned} \tag{5.15}$$

Note that another advantage of the Metropolis algorithm is that we only need to know the probability distribution $P(U)$ up to a proportianality factor, as it only appears in P_A as $P(U')/P(U)$. The algorithm is thus very well suited for our case, where we want to consider configurations distributed according to $\propto e^{-S_G[U]}$.

When constructing $T_0(U'|U)$, as we will do later, we make sure that $T_0(U'|U) = T_0(U|U')$. Then the detailed balance condition is also fulfilled, even if $T_0(U'|U) \geq 0$. The probability of acceptance becomes

$$P_A = \min\left\{1, e^{-\Delta S}\right\}, \text{ where } \Delta S = S_G[U'] - S_G[U]. \tag{5.16}$$

5.3 Implementation

In the previous section we have become acquainted with the Metropilos algorithm, which updates configuration U_{n-1} to U_n. Each update consists of two steps: a candidate configuration is proposed according to T_0, which is accepted with probability P_A, see Eq. 5.16. In this way a Markov chain of configurations is generated according to the correct probability distribution.

In this section I will show how the Metropolis algorithm is implemented in the script that I use, which can be found on the webpage [12].

In summary: one Metropolis update changes only one link variable. This will turn out to allow for a very efficient algorithm, which updates all links in each space time direction μ several times. Every link variable is thus addressed. This procedure is repeated several times, before calculating the next value of the observable. I note here that in calculating the expectation value Eq. 5.2, the observable is immediately calculated and stored, rather than storing all configuration and calculating the observable afterwards.

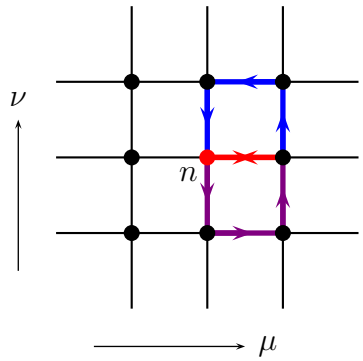

Figure 5.1: Upon changing $U_\mu(n)$ (red), two plaquettes are affected in each of the three remaining space time directions ν: $U_{\mu\nu}(n)$ (blue) and $U_{\mu\nu}(n-\hat{\nu})$ (violet).

5.3.1 Update one link variable

We consider the Metropolis update of one link variable $U_\mu(n)$. The candidate (**step 1**) is obtained by multiplying by $X_{(\mu,n)}$, a random element of the gauge group.

$$U_\mu(n) \to U'_\mu(n) = X_{(\mu,n)} U_\mu(n) \tag{5.17}$$

The labels (μ, n) merely indicate that it multiplies $U_\mu(n)$. Details on how $X_{(\mu,n)}$ is generated can be found in appendix A.1.

In order to calculate the probability P_A that $U'_\mu(n)$ is accepted (**step 2**) we need to calculate how the action changes. Remember that the action for a configuration U, consisting of all link variables $U_\mu(n)$ is given by (Eq. 3.21)

$$S_G[U] = \frac{\beta}{3} \sum_n \sum_{\mu<\nu} \text{Re tr} \left[\mathbf{1} - U_{\mu\nu}(n)\right], \tag{5.18}$$

with $U_{\mu\nu}(n)$ the plaquettes: Eq. 3.20 and Fig. 3.3.

Upon changing one link variable $U_\mu(n)$, only six plaquettes are affected: $U_{\mu\nu}(n)$ and $U_{\mu\nu}(n-\hat{\nu})$ for the remaining $d-1$ space time directions ν, see Fig. 5.1. The rest stays the same. Now note that $\text{Re tr}\left[U_{\nu\mu}\right](n-\hat{\nu}) = \text{Re tr}\left[U^\dagger_{\mu\nu}\right](n-\hat{\nu}) = \text{Re tr}\left[U_{\nu\mu}\right](n-\hat{\nu})$. We thus find that

$$\Delta S = \frac{-\beta}{3} \text{Re tr}\left[(U'_\mu(n) - U_\mu(n)) A_{(\mu,n)}\right], \tag{5.19}$$

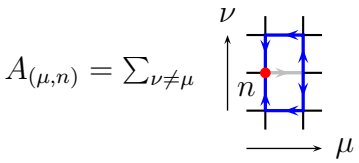

Figure 5.2: $A_{(\mu,n)}$ is the sum over remaining space time directions ν of the unaffected link variables of $U_{\mu\nu(n)}$ and $U^\dagger_{\mu\nu}(n-\hat{\nu})$. The link variable $U_\mu(n)$ is indicated in grey.

where $A_{(\mu,n)}$, called staple, is the sum over the unaffected parts of $U_{\mu\nu}(n)$ and $U_{\mu\nu}(n-\hat{\nu})$:

$$A_{(\mu,n)} = \sum_{\nu\neq\mu} U_\nu(n+\hat{\mu})U^\dagger_\mu(n+\hat{\nu})U^\dagger_\nu(n) + U_{-\nu}(n+\hat{\mu})U^\dagger_\mu(n-\hat{\nu})U^\dagger_{-\nu}(n), \quad (5.20)$$

or pictorially, see Fig. 5.2.

Finally, our link variable $U_\mu(n)$ is replaced by $U'_\mu(n)$, with probability $\min\left\{1, e^{-\Delta S}\right\}$.

In the next section we will see that there is an efficient way to update all link variables (several times).

5.3.2 Update all link variables

In the previous section we saw how we can implement the Metropolis changing one link variable. In this section we discuss the algorithm we use, updating all link variables in an efficient way.

A clever trick for dealing with many link variables at once is to divide the lattice in two sub lattices as follows. We define a lattice point $n = (n_1, n_2, n_3, n_4)^T$ to be even (odd) if the sum $n_1 + \ldots + n_4$ is even (odd). Pictorially this means that starting from 0 every second lattice point along an arbitrary path is even, see 5.3.

Remember that changing one link variable $U_\mu(n)$, six plaquettes are effected: 2 in each of the 3 remaining space time directions ν. If we now change the link variables starting on *all* even (odd) sites, then the corresponding staples do not overlap, see 5.4. This allows us to calculate $A_{(\mu,n)}$ for all even (odd) sites, for the given direction μ, and thus to update all the link variables using in particular Eqs. 5.19 and 5.20.

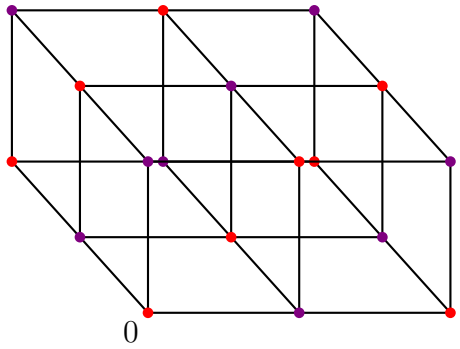

Figure 5.3: The even (odd) lattice sites are depicted red (violet).

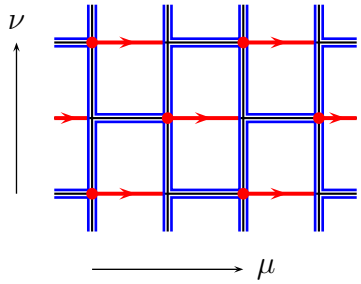

Figure 5.4: The staples (blue), corresponding to the link variables $U_\mu(n)$ (red arrows) starting on even sites (red spots), do not overlap. We can thus collect them all at once. Note that the blue arrows are suppressed, see Fig. 5.2.

In order to update the all link variables, we do the following. Note that that the above procedure updates all link variables starting on even (odd) sites in one space time direction μ. As calculating $A_{(\mu,n)}$ is relatively costly, we update several times for each space time direction, for firstly the even, then the odd sub lattice. This ensures that the whole lattice is updated.

Finally we repeat updating the whole lattice several times before calculating the Wilson loop.

To summarise: we have seen how the our script changes all the link variables using the Metropolis algorithm. This produces a Markov chain of correctly distributed configurations, which allows us to calculate the expectation value Eq. 5.2. In the next chapter I present my numerical results for both $\langle P \rangle_{\beta_T}$ and individual $P[U_i]$'s.

Chapter 6

Numerical results: Phase transition

In this chapter I present the results for my numerical calculation of the order parameter $\langle P \rangle_{\beta_T}$ defined in section 4.1. The data has been obtained from simulation on lattices of size $N^3 \times N_t$, for $N_t = 4$ and $N = 8$ as well as $N = 14$.

Remember (chapter 5) that expectation values of an observable O are calculated as the average over $O[U_i]$, with U_i the configurations generated in a Markov chain. I calculate the order parameter $\langle P \rangle_{\beta_T}$, with $P[U_i]$ the spacial average of the Polyakov loops

$$P = \frac{1}{N^3} \sum_{\mathbf{m} \in \Lambda^3} P(m), \tag{6.1}$$

where the Polyakov loop given by 4.4.

We have seen that $\langle P \rangle_{\beta_T}$ probes the confinement of a single quark:

$$\begin{aligned} \langle P \rangle_{\beta_T} &= 0 \text{ confinement} \\ \langle P \rangle_{\beta_T} &\neq 0 \text{ deconfinement.} \end{aligned} \tag{6.2}$$

I show results for the *pass by pass*, i.e. the individual values, of $P[U_i]$ and $\langle |P| \rangle_{\beta_T}$ for different values of the inverse coupling β. The pass by pass results are interesting, as each step in the MC simulation (using the Metropolis algorithm, with a sufficiently high number of hits) is equivalent to the exposure of the links to a heat bath [13] and thus yields thermal fluctuations. We will see that values

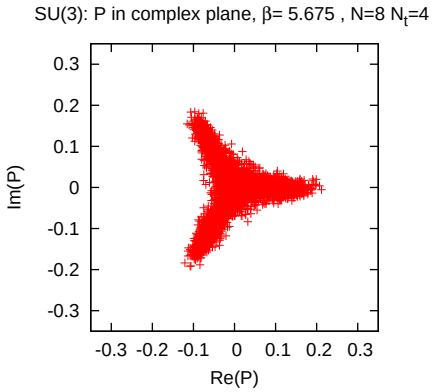

Figure 6.1: Symmetry breaking results in values $P = z|P|$.

of P are distributed following the roots $z = 1, e^{\pm\frac{2\pi i}{3}}$ and that there is *tunnelling* between the corresponding "states". For this reason I consider $|P|$ rather than P for the thermal average.

The results for $\langle|P|\rangle_{\beta_T}$ show a *phase transition* as a function of the inverse coupling β. It is believed that this phase transition is of first order [14], and I will show compatible signs of coexisting states near the phase transition. I compare the results for the two different lattice sizes.

6.1 Pass by pass

In Fig. 6.1, 3000 pass by pass values $P[U_i]$ are depicted in the complex plane for $N = 8$ and $N_t = 4$. Remember that Z_3 symmetry breaking results in values $P = z|P|$. Hence the distribution in complex plane. Typically P fluctuates around a fixed value unless it tunnels to another state. We will see that $\beta = 5.675$ is close to the phase transition, where there is more tunnelling between the states. This is typical for the smaller lattice with $N = 8$.

An explicit example of tunnelling is given in Fig. 6.2, where Re (P) as well as Im (P) are given for 1000 passes. After roughly 800 passes, we observe tunnelling from $P = e^{\frac{-2\pi i}{3}}|P|$ to the $P = |P|$ state.

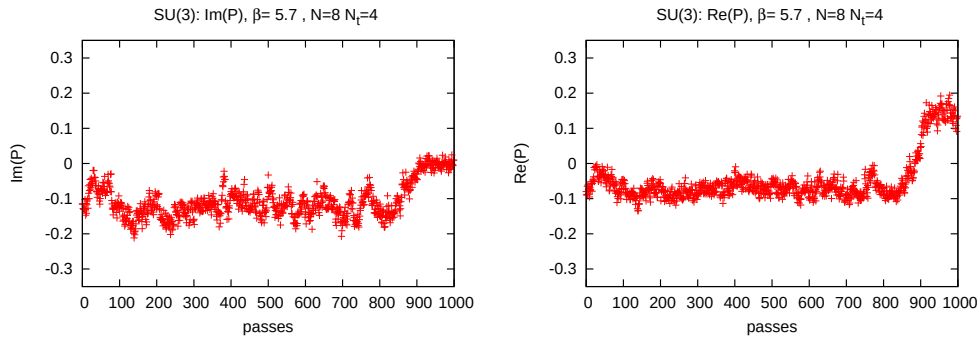

(a) Imaginary (b) Real

Figure 6.2: From Im (P) 6.2a and Re (P) 6.2b we observe tunnelling from $P = e^{\frac{-2\pi i}{3}}|P|$ to the $P = |P|$ state, after approximately 800 passes.

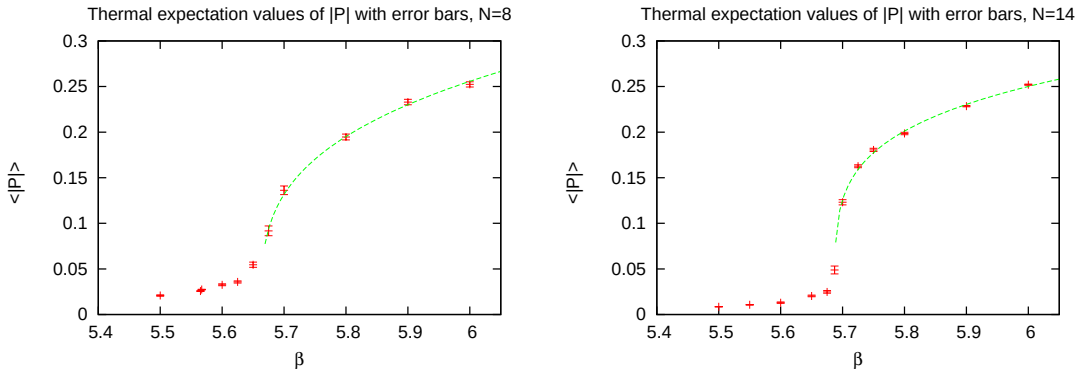

(a) $N = 8$ (b) $N = 14$

Figure 6.3: The red crosses show thermal expectation values $|P|$ for different values of β on $N^3 \times N_t$ lattices with $N = 8$ and $= 14N$. The error bars are obtained using Eq. B.6. The correlation length is large at the phase transition and more measurement have been taken accordingly. The green line shows a fit to Eq. 6.3, of the data for β's above the phase transition. Based on this fit we find the critical values $\beta_c = 5.663$ ($\beta_c = 5.687$) for $N = 8$ ($N = 14$). The phase transition is sharper for the $N = 14$ lattice.

6.2 Phase transition

This section contains the most important results of this work. Results for $|P|$, with $N = 8$ ($N = 14$), versus the inverse coupling β are plotted in Figs. 6.3a (6.3b).

For each value of β the average of $|P|$, c.f. Eq. 5.2, was taken over a large number (200-5000) of passes. The data was collected in several runs. The error bar was calculated using the autocorrelation time (Eq. B.6) where the autocorrelation time was calculated from the largest run. Near the phase transition the autocorrelation time is larger: up to 86 for $N = 14$ at $\beta = 5.687$. Accordingly more measurements (4000-5000) have been taken. To appreciate this, one should realise that 4000 measurements at the $N = 14$ lattice take about 12 hours on an ordinary machine.

When configurations are generated for a given β, it takes a certain amount of steps to reach thermal equilibrium. To facilitate this, for each β the last configuration in the Markov chain was used as the first configuration for the next β. The passes needed to come to equilibrium have been removed from the data used in Figs. 6.3a and 6.3b. Near the phase transition it takes longer to come to equilibrium, e.g. for $\beta = 5.700$ and $N = 14$ it takes 300 passes.

The important observation is that a *phase transition* takes place from the symmetric or confined phase to a deconfined phase after some critical β_c. So physically there is a critical temperature T_c above which single heavy quarks get deconfined. The green line in Figs. 6.3a and 6.3b shows a fit of the function

$$f(\beta) = C\,(\beta - \beta_c)^{\alpha} \tag{6.3}$$

to the data above the critical phase transition, from which we extract the critical β_c. We find $\beta_c = 5.663$ ($\beta_c = 5.687$) for $N = 8$ ($N = 14$). Using the formula for $a(\beta)$, Eq. 4.20, we find a corresponding temperatures of $T_c = 268$ ($T_c = 285$). It is not the aim of this work to do a precise measurement of β_c or T_c. To obtain uncertainties for these quantities, statistical tools like jackknife [15] would be suggested.

Note that the phase transition is sharper for the $N = 14$ than the $N = 8$

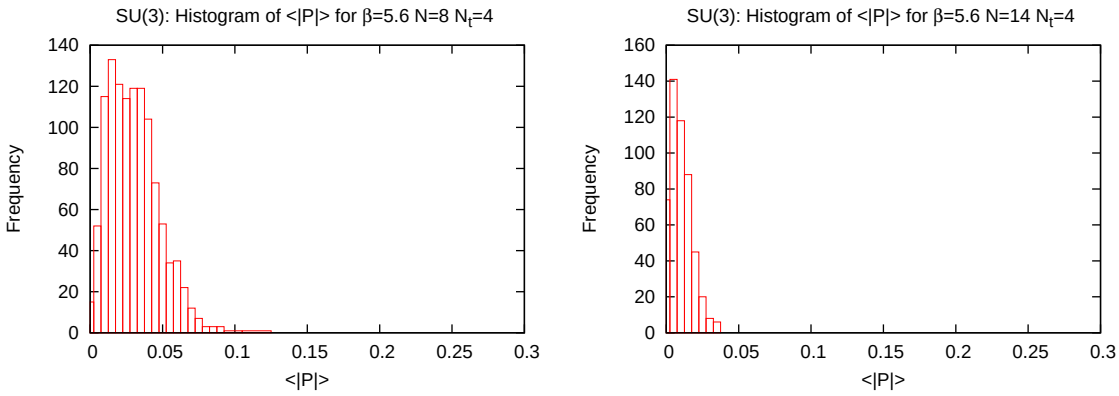

(a) (b)

Figure 6.4: The histograms for $|P|$ for $N = 8$ ($N = 14$), Fig. 6.4a (6.4b) at $\beta = 5.600$, i.e. below β_c, show a cleaner distribution around zero for the $N = 14$. This is more generally true for other values of β.

lattice. This is an effect of using a bigger lattice. Consider the histogram for $|P|$, Fig. 6.4, for $\beta = 5.600$, which is below the phase transition. The $N = 14$ lattice gives a cleaner distribution of $|P|$ around zero. This is more generally true for all values of β. Therefore, if one wants to extend this analysis, larger lattices are required.

6.3 Nature phase transition

It is suggested that the phase transition for our cause of $SU(3)$ pure gauge theory in $3+1$ dimensions is first order [14]. One of the signals compatible with this, are hints of a coexisting phase at the phase transition. The best evidence was found at $\beta = 5.687$. The histogram in Fig. 6.5a hints that the links appear in two types of states with, i.e. with different $|P|$. More convincing is perhaps Fig. 6.5b, in which $|P|$ is shown for the first 1000 of the 4000 passes which were used for the histogram. From this figure it can be seen that tunnelling is more rapid than the duration of the "stay" in the small $|P|$ state (roughly passes 400-700). Further investigation could be done by probing more values of β to reach a point where the two phase occur equally often. Then one should move on to bigger lattices. If there really are coexisting phases an the phase transition, then the peaks should

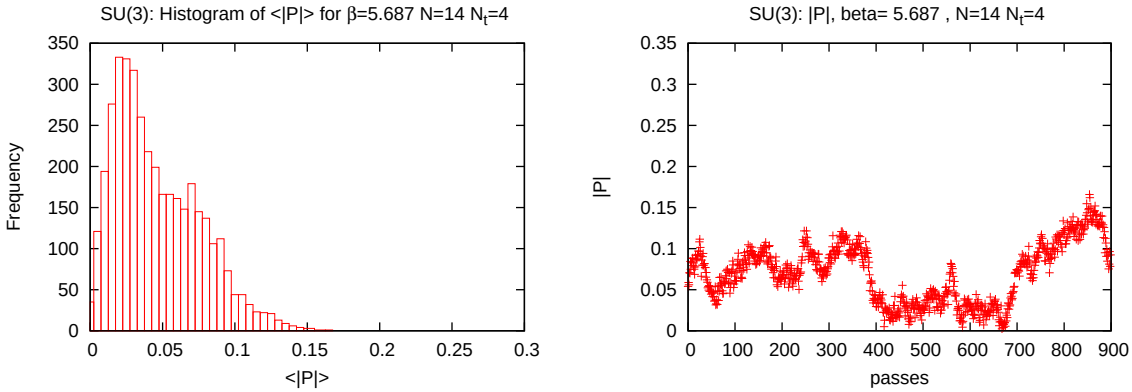

(a) (b)

Figure 6.5: The histogram Fig. 6.5a shows a hint of a two coexisting phases, corresponding to different $|P|$. Fig. 6.5b shows the first 1000 of the 4000 passes, used to build up the histogram. Between 400 and 700 we see tunnelling to a state of small $|P|$, which remains for a longer time than would be expected from tunnelling immediately to other states $P = z|P|$. It was confirmed that in the complex plane this P fluctuated around $e^{-\frac{2\pi i}{3}}|P|$, before moving to small $|P|$, and around $1|P|$ after.

become sharper and the number of passes with $|P|$ between the peaks should vanish.

This concludes my results. We have seen a phase transition from the symmetric, confined phase to a deconfined phase, where the centre symmetry is broken. It turns out that the $N = 14$ shows a sharper phase transition and has cleaner distributions for the individual values of $|P|$. Finally we have seen a sign of coexisting phases near the phase transition, which is compatible with the claim that the phase transition is of first order.

Chapter 7

Conclusions

The main aim of this thesis is to investigate the phase transition in the confinement of the single heavy quark at finite temperature.

This has been done using by numerically calculating the order parameter $\langle P \rangle_{\beta_T}$: the thermal expectation value of the Polyakov loop. I have explained how to calculate thermal expectation values the Polyakov loop on the lattice, namely taking the its average over configurations generated in a Markov Chain. We have seen that the Markov chain is generated in a Monte Carlo simulation using the Metropolis algorithm.

A crucial ingredient in the interpretation of the phase transition is the centre symmetry, which predicts that values for the Polyakov loop are given by $P = z|P|$, with $z = 1, e^{\pm \frac{2\pi i}{3}}$.

I have calculated the order parameter on two $N^3 \times N_t$ lattices, with $N = 8$ and $N = 14$, for different values of the bare (inverse) coupling β, corresponding to different temperatures. The values of P for individual Monte Carlo steps indeed show a distribution in the complex plane expected from the centre symmetry. Tunnelling is observed between the different states corresponding to z. For the respective lattices I found the critical $\beta_c = 5.663$ and $\beta_c = 5.687$, above which $\langle |P| \rangle_{\beta_T} \neq 0$, i.e the quark gets deconfined. The phase transition is sharper for the $N = 14$ lattice and the distribution of $|P|$ is cleaner. This is due to the bigger size of the lattice.

Finally I have discussed the order of the phase transition. It is suggested in the literature that it should be of first order. On the $N = 14$ lattice I find signs

of a two coexisting phases at the critical β, which is compatible with this.

To extend the analysis presented in this work, I suggest that more values for β near the phase transition should be investigated on the $N = 14$ lattice. Also, in order to confirm the coexisting phases, one would have to move to a bigger lattice and see if the signals become cleaner. One could also perform statistical checks to give estimates for the error made in the determination of β_c.

Appendix A

Utilities for program

In this appendix I complete the description of the script (section 5.3) that I have used. I specify how obtain the matrices $X_{(\mu,n)}$, used to compute a candidate $U'_\mu(n) = X_{(\mu,n)}U_\mu(n)$ (Eq. 5.17), are calculated.

A.1 Transition matrix

Remember that we update half of the link variables in one space time direction at once, namely of the even (odd) sites. So defining N_S the number of sites, we need $N_S/2$ matrices.

In the following $n = 0, \ldots, N_S/2$. The program I use generates $N_S/2$ elements of the gauge group Y_n. Then the matrix $X_{(\mu,n)} = Y^{(\dagger)}_{n+r}$, where r is chosen randomly in $[0, \ldots, \frac{N_S}{2}]$ and $(\dagger)$ indicates that Y is randomly inverted with probability $\frac{1}{2}$, i.e. the hermetian conjugated. The latter ensures that each X is as likely to occur as $X^\dagger$, which corresponds to demanding that $T(U|U') = T(U'|U)$.

The Y_n matrices are generated using the following algorithm. It generates random $SU(3)$ matrices with a bias to the identity (which depends on β) and shuffles and modifies them in a Metropolis-inspired fashion.

- **Generate $2 \times N_S/2$ random elements of $SU(3)$.** Define $R_{1,n}, R_{2,n} = \frac{\beta}{3}\mathbf{1} + R'[-\frac{1}{2}, \frac{1}{2}]$, where R' is a matrix containing elements uniformally distributed in $[-\frac{1}{2}, \frac{1}{2}]$. In order to make group elements of these random matrices, they are projected on the elements of $SU(3)$: $R_{1,n}, R_{2,n} \to Z_{1,n}, Z_{2,n}$,

see section A.1.1.

- **Modify and shuffle $Z_{1,n}$ and $Z_{2,n}$: repeat** $50\times$
  - $S_n = Z^{(\dagger)}_{1,n+r}$
  - $Z_{1,n} \to Z'_{1,n} = Z_{2,n} S_n$
  - $Z_{2,n} \to Z'_{2,n} = Z'_{1,n}$ with probability $\min\left\{1, e^{\frac{\beta}{3}\mathrm{tr}\left[Z'_{1,n} - Z_{2,n}\right]}\right\}$ and is unchanged otherwise.
  - Now set $Z_{1,n} = Z'_{2,n}$ and $Z_{2,n} = S_n$
  - Project elements of $Z_{1,n}$ on $SU(3)$
- We finally set $Y_n = Z_{1,n}$.

A.1.1 Project matrix on $SU(3)$

As we saw in section A.1, we sometime need to project matrices on our gauge group $SU(3)$. This is done as follows. Let M be the matrix, which is to be projected. We call its first two rows $\mathbf{u}$ and $\mathbf{v}$. Now normalise $\mathbf{u} \to \mathbf{u}' = \mathbf{u}|\mathbf{u}|$. Via Gramm SCHMIDT???, we find the orthonormal second row $\mathbf{v} \to \mathbf{v}' = \mathbf{w}/|\mathbf{w}|$, where $\mathbf{w} = \mathbf{v} - (\mathbf{v} \cdot \mathbf{u}'^*)\mathbf{u}'$. The third row is given by $\mathbf{u}'^* \times \mathbf{v}'^*$.

We thus end up with the matrix

$$M \to \begin{pmatrix} \mathbf{u}' \\ \mathbf{v}' \\ \mathbf{u}'^* \times \mathbf{v}'^* \end{pmatrix}, \tag{A.1}$$

which is indeed an element of $SU(3)$.

Appendix B

Calculation of error bars

I calculate thermal expectation values $\langle O \rangle_{\beta_T}$ of some observable O, e.g. the Polyakov loop P. To do so I generate a Markov Chain of N_m configurations U_i and calculate $O(U_i) \equiv o_i$, see chapter 5. Then the thermal expectation value is approximated by, c.f. Eq. 5.2

$$\langle O \rangle_{\beta_T} = \frac{1}{N_m} \sum_{i=1}^{N_m} o_i. \tag{B.1}$$

We want to estimate by how much $\langle O \rangle_{\beta_T}$ is wrong, i.e. determine its standard deviation $\sigma_{\langle O \rangle_{\beta_T}}$. In the following I summarise how to calculate this. An actual explanation can be found in [4], chapter 4.

Assume that o_i is chosen according to a random variable X, with standard deviation σ_X. If $\langle O \rangle_{\beta_T}$ was the result of N_{ind} *independent* "measurements", then the standard deviation $\sigma_{\langle O \rangle_{\beta_T}}$ for $\langle O \rangle_{\beta_T}$ would be given by

$$\sigma_{\langle O \rangle_{\beta_T}} = \frac{\sigma_X}{\sqrt{N_{ind}}}, \tag{B.2}$$

where we approximate the square of the standard deviation σ_X^2 by

$$\sigma_X^2 = \frac{1}{N_m} \sum_{i=1}^{N_m} (o_i - \langle O \rangle_{\beta_T})^2. \tag{B.3}$$

However, in general the o_i's are correlated, because the subsequent configu-

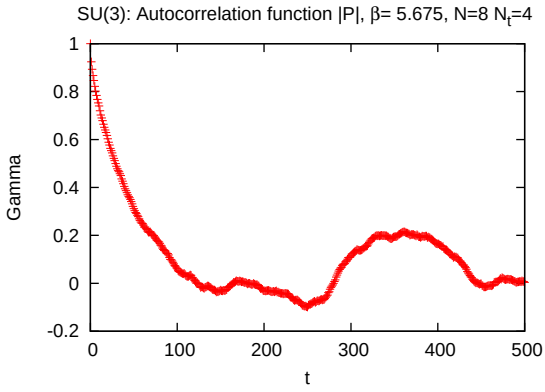

Figure B.1: Normalised autocorrelation function for $|P|$ at the phase transition. This is where we find the largest autocorrelation time. Even in this case, in the beginning it looks like an exponentially dropping function. The autocorrelation time τ is determined by the first t for which $\Gamma(t) < \frac{1}{e}$.

rations in the Markov chain are correlated. A measure for this is given by the *autocorrelation time* τ defined as follows. We define the *autocorrelation function* as

$$C(t) = \frac{1}{N_m - t} \sum_{i=1}^{N_m - t} (o_i - \langle O \rangle_{\beta_T})(o_{i+t} - \langle O \rangle_{\beta_T}). \tag{B.4}$$

I use the result that normalising autocorrelation function, i.e. dividing $C(t)$ by $C(0)$, gives approximately an exponentially dropping function

$$\Gamma(t) = \frac{C(t)}{C(0)} \approx \exp\left(-\frac{t}{\tau}\right), \tag{B.5}$$

where τ is the autocorrelation time. In Fig. B.1 an example is given of $\Gamma(t)$, to illustrate that exponential decay is a plausible assumption. In my analysis I simply determine τ by the first value t for which $\Gamma(t) < \frac{1}{e}$.

Then I assume measurements to be independent after a time τ so that $N_{ind} = \frac{N_m}{\tau}$. Putting together Eqs. B.2, B.3 I thus get my expression for the uncertainty in $\langle O \rangle_{\beta_T}$

$$\boxed{\sigma_{\langle O \rangle_{\beta_T}} = \sqrt{\frac{\tau}{N_m}} \sigma_X}. \tag{B.6}$$

References

[1] A.M. Polyakov. Thermal properties of gauge fields and quark liberation. *Physics Letters B*, 72(4):477 – 480, 1978. 1

[2] L. D. McLerran and B. Svetitsky. Quark liberation at high temperature: A monte carlo study of su(2) gauge theory. *Phys. Rev. D*, 24:450–460, Jul 1981. 1, 16, 17

[3] M. E. Peskin and D. V. Schroeder. An Introduction to quantum field theory. 1995. 3

[4] C. Gattringer and C. B. Lang. Quantum chromodynamics on the lattice. *Lect.Notes Phys.*, 788:1–211, 2010. 4, 22, 42

[5] D. J. Gross, R. D. Pisarski, and L. G. Yaffe. QCD and Instantons at Finite Temperature. *Rev.Mod.Phys.*, 53:43, 1981. 6, 7, 20

[6] M. Göckeler and T. Schücker. *Differential Geometry, Gauge Theories, and Gravity*. Cambridge Monographs on Mathematical Physics. Cambridge University Press, October 1989. 8

[7] K. G. Wilson. Confinement of quarks. *Phys. Rev. D*, 10:2445–2459, Oct 1974. 14

[8] L. McLerran. Strongly interacting matter at very high energy density: Three lectures in zakopane. *Act. Phys. Pol. B*, 41(12):799–2826, Dec. 2010. 18

[9] S. Necco and Sommer R. The nf=0 heavy quark potential from short to intermediate distances. *Nuclear Physics B*, 622(1-2):328 – 346, 2002. 21

[10] R. Sommer. A new way to set the energy scale in lattice gauge theories and its application to the static force and σ_s in su (2) yang-mills theory. *Nuclear Physics B*, 411(2-3):839 – 854, 1994. 21

[11] M. Creutz. Monte carlo study of quantized su(2) gauge theory. *Phys. Rev. D*, 21:2308–2315, Apr 1980. 21

[12] M. Creutz. http://latticeguy.net/lattice.html. 22, 27

[13] M. Creutz. Overrelaxation and monte carlo simulation. *Phys. Rev. D*, 36:515–519, Jul 1987. 32

[14] L. G. Yaffe and B. Svetitsky. First-order phase transition in the su(3) gauge theory at finite temperature. *Phys. Rev. D*, 26:963–965, Aug 1982. 33, 36

[15] M. E. J. Newman and G. T. Barkema. *Monte Carlo Methods in Statistical Physics*. Oxford University Press, Mar 1999. 35